Microscopic coupled-channel study of the five-nucleon system with the resonating-group method*

F. S. Chwieroth,† Y. C. Tang, and D. R. Thompson
School of Physics and Astronomy, University of Minnesota, Minneapolis, Minnesota 55455
(Received 10 September 1973)

A coupled-channel study of the five-nucleon system is performed with the resonating-group method. The channels which are explicitly considered are the $d+{}^3\mathrm{He}$ (or $d+{}^3\mathrm{H}$) and the $p+\alpha$ (or $n+\alpha$) channels. Three- and more-body breakup channels are not included in the calculation, but their effects are crudely taken into account by the introduction of phenomenological imaginary potentials into the formulation. The nucleon-nucleon potential used is purely central, but does yield correct values for the two-nucleon effective-range parameters. Differential scattering and reaction cross sections are calculated at various energies. The result shows that for the $d+{}^3\mathrm{He}$ and $p+\alpha$ differential scattering cross sections, the calculated values in general agree quite well with the experimental data. For the $d+{}^3\mathrm{He} \rightleftarrows p+\alpha$ differential reaction cross sections, the comparison between theory and experiment is somewhat less satisfactory. Although the general features of the experimental angular distributions are well reproduced, the magnitude of the calculated cross section is somewhat too low.

[NUCLEAR REACTIONS $^3\mathrm{He}(d,d)$, $^3\mathrm{He}(d,p)$, $^4\mathrm{He}(p,d)$, $^4\mathrm{He}(p,p)$, $E=0$–50 MeV; calculated $\sigma(\theta)$. Resonating-group method; coupled-channel calculation.]

I. INTRODUCTION

In the past several years, we have used the single-channel resonating-group method to study a number of light nuclear systems.[1] When used together with a phenomenological imaginary potential to take approximate account of reaction effects, it has been found that quite satisfactory agreement with experimental differential scattering cross-section results can be obtained in all cases which have been considered.

The success of these single-channel studies indicates to us that more elaborate calculations with the resonating-group method are now warranted. In this investigation, we shall therefore make a coupled-channel study of the five-nucleon system. Specifically, the channels which will be considered are the $d+{}^3\mathrm{He}$ (or $d+{}^3\mathrm{H}$) and the $p+\alpha$ (or $n+\alpha$) channels. Three- and more-body breakup channels will not be included in this calculation; they will be taken into account only in a crude manner as described below.

The purpose of this investigation is twofold. First, we wish to learn the influence of a second channel on elastic scattering in the first channel. *A priori*, it seems plausible that in the case of $d+{}^3\mathrm{He}$ elastic scattering, where the two clusters involved are easily deformable, the addition of the $p+\alpha$ channel should have a significant effect. On the other hand, since the α cluster has a rather low compressibility, the addition of a second channel should have rather little influence on $p+\alpha$ elastic scattering. Second, we wish to know the usefulness of the resonating-group approach in studying reactions in light nuclear systems. This will be achieved by making a detailed comparison of calculated differential reaction cross sections with existing experimental data. In addition, it should be mentioned that the results obtained here can also be used to make a careful study of reaction mechanisms. This will be the subject of a future investigation.

Coupled-channel resonating-group calculations for the five-nucleon system have previously been performed by Laskar *et al.*,[2] and by Heiss and Hackenbroich.[3] Although the investigation of Heiss and Hackenbroich was a rather careful one, only partial waves up to $l=2$ were included; hence for the five-nucleon system, which involves diffuse clusters, a comparison with experimental cross-section data is not possible even at energies of only a few MeV. In addition, these previous calculations did not account for many-body breakup reaction channels. As has been found experimentally,[4] reactions proceed mainly through three- or more-particle channels, if these channels are open. Thus, since in the mass-5 system these channels are open already at energies rather close to the $d+{}^3\mathrm{He}$ threshold, it is necessary to account for them in some way. In this calculation, as in previous single-channel studies,[1] we shall simply approximate these channels by the introduction of phenomenological imaginary potentials into the resonating-group formulation.

In the next section, a brief formulation of the problem is given. In Sec. III, we present the calculated S matrix and discuss the level structures of ^{5}He and ^{5}Li. We compare the calculated and experimental results for the differential elastic scattering cross section in Sec. IV and for the differential reaction cross section in Sec. V. Finally, in Sec. VI, concluding remarks are made.

II. FORMULATION

Since a detailed discussion of the formulation of the two-channel problem is given elsewhere,[5] we shall present only a brief formulation here.

The wave function for the five-nucleon system is assumed as

$$\Psi_2 = \mathcal{A}[N_f^{-1/2}\phi_3\phi_d F(\vec{R}_3 - \vec{R}_d)\xi_f(\sigma,\tau) + N_g^{-1/2}\phi_\alpha G(\vec{R}_\alpha - \vec{R}_N)\xi_g(\sigma,\tau)] \quad (1)$$

in the spin-$\frac{1}{2}$ state, and

$$\Psi_4 = \mathcal{A}[N_h^{-1/2}\phi_3\phi_d H(\vec{R}_3 - \vec{R}_d)\xi_h(\sigma,\tau)] \quad (2)$$

in the spin-$\frac{3}{2}$ state. The subscript 2 or 4 of the function Ψ denotes the channel-spin multiplicity $(2s+1)$, with s denoting the channel-spin angular momentum quantum number of the system. It is permissible to consider the two spin states as uncoupled here, since we shall employ a central nucleon-nucleon potential in our calculation.

Because of the adoption of a purely central nucleon-nucleon potential, the spin-$\frac{3}{2}$ state of the $d+^3$He system will not be affected by the addition of the $p+\alpha$ channel. Therefore, since it has already been considered in detail in our previous single-channel study[1] of the $d+^3$He system, we shall not further discuss it here.

In Eq. (1), the symbol $\mathcal{A}$ denotes the antisymmetrization operator and the functions ξ_f and ξ_g denote the appropriate spin-isospin functions. The functions ϕ_3, ϕ_d, and ϕ_α describe the spatial behavior of the three-nucleon cluster (either ^{3}He or ^{3}H), the deuteron cluster, and the α cluster, respectively, while the functions $F(\vec{R}_3 - \vec{R}_d)$ and $G(\vec{R}_\alpha - \vec{R}_N)$ describe the relative motion of the clusters in each channel. The quantities $1/\sqrt{N_f}$ and $1/\sqrt{N_g}$ are included so that the cluster internal functions are normalized to unity. Here and throughout this paper, we use the subscripts f and g to refer to the $d+^3$He (or $d+^3$H) and $p+\alpha$ (or $n+\alpha$) channels, respectively.

The functions ϕ_α and ϕ_3 are assumed as

$$\phi_\alpha = \exp\left[-\tfrac{1}{2}\alpha\sum_{j=1}^{4}(\vec{r}_j - \vec{R}_\alpha)^2\right] \quad (3)$$

and

$$\phi_3 = \exp\left[-\tfrac{1}{2}\gamma\sum_{j=1}^{3}(\vec{r}_j - \vec{R}_3)^2\right], \quad (4)$$

with $\vec{R}_\alpha$ and $\vec{R}_3$ being the position vectors of the center of mass of the α cluster and the three-nucleon cluster, respectively. The parameters α and γ are chosen to yield the correct rms matter radii for the respective nuclei[6]; they are

$$\alpha = 0.514 \text{ fm}^{-2} \quad (5)$$

and

$$\gamma = 0.378 \text{ fm}^{-2} \text{ for } ^3\text{H}; \quad = 0.367 \text{ fm}^{-2} \text{ for } ^3\text{He}. \quad (6)$$

For the diffuse deuteron cluster, it is necessary to use a more complicated cluster function

$$\phi_d = \sum_{i=1}^{3} A_i \exp\left[-\tfrac{1}{2}\alpha_i\sum_{j=4}^{5}(\vec{r}_j - \vec{R}_d)^2\right], \quad (7)$$

where $\vec{R}_d$ denotes the position vector of the center of mass of the deuteron cluster. The parameters A_i and α_i are determined by minimizing the expectation value of the deuteron Hamiltonian; the result is[7]

$$A_1 = 1.000, \quad \alpha_1 = 0.072\,84 \text{ fm}^{-2},$$
$$A_2 = 3.631, \quad \alpha_2 = 0.3657 \text{ fm}^{-2}, \quad (8)$$
$$A_3 = 5.746, \quad \alpha_3 = 1.4696 \text{ fm}^{-2}.$$

With the wave functions of Eqs. (3)–(8), we obtain a binding energy of 2.20 MeV for the deuteron cluster, 3.96 MeV for the ^{3}He cluster, 4.79 MeV for the ^{3}H cluster, and 26.61 MeV for the α cluster, as compared to the experimental values of 2.22, 7.72, 8.48, and 28.3 MeV, respectively.

The one-Gaussian functions ϕ_α and ϕ_3 reproduce fairly well the experimental form factors in the low-momentum-transfer region, and their use in single-channel calculations[6] has been found to be quite adequate. In the present two-channel calculation, however, the lack of close agreement between calculated and experimental cluster binding energies does lead to a discrepancy of 2.1 MeV in the $d+^3$He threshold energy. As a consequence, we will not be able to make any comparison with experiment for the reaction $\alpha(p,d)^3$He at energies close to the $d+^3$He reaction threshold. For the inverse reaction ^{3}He$(d,p)\alpha$, however, the defect in the calculated differential reaction cross section caused by this discrepancy in the threshold energy should be relatively minor and a detailed comparison with experiment can be made.

The relative-motion functions $F(\vec{R}_f)$ and $G(\vec{R}_g)$

are determined from the projection equation

$$\langle \delta\Psi_2 | H - E' | \Psi_2 \rangle = 0 , \tag{9}$$

where E' is the total energy, composed of the internal energies (E_α, E_3, and E_d) of the clusters and the relative energies (E_f and E_g) in the c.m. system; that is,

$$\begin{aligned} E' &= E_\alpha + E_g \\ &= E_3 + E_d + E_f . \end{aligned} \tag{10}$$

Also, H is the Hamiltonian operator, given by

$$H = -\frac{\hbar^2}{2M} \sum_{i=1}^{5} \nabla_i^2 + \sum_{i>j=1}^{5} V_{ij} , \tag{11}$$

where the nucleon-nucleon potential V_{ij} is taken as

$$\begin{aligned} V_{ij} = &[\tfrac{1}{2}(1 + P_{ij}^{\sigma}) V_{ij}^{t} + \tfrac{1}{2}(1 - P_{ij}^{\sigma}) V_{ij}^{s}] \\ &\times [\tfrac{1}{2}u + \tfrac{1}{2}(2 - u) P_{ij}^{r}] + \frac{e^2}{r_{ij}} \frac{1 + \tau_{iz}}{2} \frac{1 + \tau_{jz}}{2} . \end{aligned} \tag{12}$$

In Eq. (12), P_{ij}^{σ} and P_{ij}^{r} are the spin- and space-exchange operators, respectively, and τ_{iz} and τ_{jz} are the z components of the isospin operators for the ith and jth particles. The quantities V_{ij}^{t} and V_{ij}^{s} denote the spin-triplet and spin-singlet nucleon-nucleon potentials, given by

$$\begin{aligned} V_{ij}^{t} &= -V_0^{t} \exp(-\kappa_t r_{ij}^2) , \\ V_{ij}^{s} &= -V_0^{s} \exp(-\kappa_s r_{ij}^2) . \end{aligned} \tag{13}$$

The constants V_0^t, κ_t, V_0^s, and κ_s are adjusted to yield the correct values for the two-nucleon effective-range parameters; they are found to be

$$\begin{aligned} V_0^t &= 66.92 \text{ MeV}, \quad \kappa_t = 0.415 \text{ fm}^{-2} , \\ V_0^s &= 29.05 \text{ MeV}, \quad \kappa_s = 0.292 \text{ fm}^{-2} . \end{aligned} \tag{14}$$

The quantity u in Eq. (12) determines the exchange mixture, with a value of $u = 1$ corresponding to the Serber mixture. It will be treated as an adjustable parameter in our calculation, and we shall discuss its choice in detail in Sec. III.

For simplicity, we have employed a nucleon-nucleon potential with no noncentral components. As a consequence, there is no coupling between the $d + {}^3\text{He}$ channel in the spin-$\frac{3}{2}$ state and the $p + \alpha$ channel. This will result in an underestimate of the differential reaction cross sections, although we tend to feel that this underestimate may not be severe enough to cause serious consequences, especially at higher energies. Also, we have learned from single-channel calculations[8] that the use of such a simplified nucleon-nucleon potential will cause the diffraction minima to be too deep. As will be seen below, this relatively minor defect does show up in our calculated scattering and reaction cross sections.

From Eq. (9), two coupled integrodifferential equations for the functions $F(\vec{R}_f)$ and $G(\vec{R}_g)$ can be derived. Upon performing a partial-wave expansion, we obtain

$$\left\{ \frac{\hbar^2}{2\mu_f} \left[\frac{d^2}{dR_f^2} - \frac{l(l+1)}{R_f^2} \right] + E_f - V_{Nf}(R_f) - V_{Cf}(R_f) \right\} f_l(R_f) = \int_0^\infty k_{ff}^{l}(R_f, R_f') f_l(R_f') dR_f' + \int_0^\infty k_{fg}^{l}(R_f, R_g') g_l(R_g') dR_g' \tag{15}$$

and

$$\left\{ \frac{\hbar^2}{2\mu_g} \left[\frac{d^2}{dR_g^2} - \frac{l(l+1)}{R_g^2} \right] + E_g - V_{Ng}(R_g) - V_{Cg}(R_g) \right\} g_l(R_g) = \int_0^\infty k_{gf}^{l}(R_g, R_f') f_l(R_f') dR_f' + \int_0^\infty k_{gg}^{l}(R_g, R_g') g_l(R_g') dR_g' , \tag{16}$$

where $f_l(R_f)$ and $g_l(R_g)$ are defined by the equations

$$F(\vec{R}_f) = \sum_{l=0}^{\infty} \frac{1}{R_f} f_l(R_f) P_l(\cos\theta_f) \tag{17}$$

and

$$G(\vec{R}_g) = \sum_{l=0}^{\infty} \frac{1}{R_g} g_l(R_g) P_l(\cos\theta_g) . \tag{18}$$

In Eqs. (15) and (16), the functions V_{Nf} (V_{Ng}) and V_{Cf} (V_{Cg}) are the direct nuclear and the direct Coulomb potentials, respectively, in the $d + {}^3\text{He}$ ($p + \alpha$) channel. The kernel functions k_{ff}^{l} and k_{gg}^{l} represent the nonlocal interactions in the $d + {}^3\text{He}$ and $p + \alpha$ channels, while the kernel functions k_{fg}^{l} and k_{gf}^{l} represent the coupling between these two channels. The expressions for these functions are very lengthy and are given in Ref. 5. Also, it should be noted that because of the Hermiticity of the Hamiltonian operator, the coupling kernels are adjoint to each other, i.e.,

$$k_{fg}^{l}(R_f, R_g) = k_{gf}^{l*}(R_g, R_f) . \tag{19}$$

Equations (15) and (16) can be solved subject to appropriate boundary conditions to yield the partial-wave S matrix. Below the $d + {}^3\text{He}$ threshold, the S matrix is a 1×1 matrix, given by

$$S_l = \exp(2i\delta_{lg}) , \tag{20}$$

where δ_{lg} is the $p+\alpha$ nuclear phase shift. Above the $d+{}^3$He threshold, the S matrix is a 2×2 matrix which is characterized by three real quantities. We choose to specify these three quantities as the $d+{}^3$He scattering phase shift δ_{lf}, the $p+\alpha$ scattering phase shift δ_{lg}, and the reflection coefficient τ_l. Thus, the S matrix is written as

$$S_l=\begin{pmatrix} S^l_{ff} & S^l_{fg} \\ S^l_{gf} & S^l_{gg} \end{pmatrix} = \begin{pmatrix} \tau_l e^{2i\delta_{lf}} & i(1-\tau_l^2)^{1/2}e^{i(\delta_{lf}+\delta_{lg})} \\ i(1-\tau_l^2)^{1/2}e^{i(\delta_{lf}+\delta_{lg})} & \tau_l e^{2i\delta_{lg}} \end{pmatrix}. \tag{21}$$

Next, we define two amplitude functions,

$$A_{\alpha\alpha}(\theta_\alpha)=-\frac{\eta_\alpha}{2k_\alpha \sin^2\frac{1}{2}\theta_\alpha}\exp[-i\eta_\alpha \ln(\sin^2\tfrac{1}{2}\theta_\alpha)+2i\sigma_{0\alpha}] + \sum_{l=0}^{\infty}\frac{2l+1}{2ik_\alpha}e^{2i\sigma_{l\alpha}}(S^l_{\alpha\alpha}-1)P_l(\cos\theta_\alpha) \tag{22}$$

and

$$A_{\alpha\beta}(\theta_\beta)=\sum_{l=0}^{\infty}\frac{2l+1}{2ik_\alpha}e^{i(\sigma_{l\alpha}+\sigma_{l\beta})}S^l_{\alpha\beta}P_l(\cos\theta_\beta). \tag{23}$$

In these equations, α denotes the incident channel and β denotes the reaction channel. The quantities k_α and $\sigma_{l\alpha}$ denote the wave number and the Coulomb phase shift, respectively, while η_α is given by

$$\eta_\alpha=\frac{zz'e^2}{\hbar v_\alpha}, \tag{24}$$

with z and z' being the atomic numbers of the two clusters, and v_α being the relative velocity of the two clusters at large separation distances. In terms of the amplitude functions, the differential cross sections for the various processes are given as follows:

$$\begin{aligned} &\frac{d\sigma}{d\Omega}(d+{}^3\text{He}\to d+{}^3\text{He})=\tfrac{2}{3}\sigma_4(\theta)+\tfrac{1}{3}|A_{ff}|^2, \\ &\frac{d\sigma}{d\Omega}(d+{}^3\text{He}\to p+\alpha)=\tfrac{1}{3}|A_{fg}|^2, \\ &\frac{d\sigma}{d\Omega}(p+\alpha\to d+{}^3\text{He})=|A_{gf}|^2, \\ &\frac{d\sigma}{d\Omega}(p+\alpha\to p+\alpha)=|A_{gg}|^2, \end{aligned} \tag{25}$$

where $\sigma_4(\theta)$ is the spin-$\frac{3}{2}$ contribution to the $d+{}^3$He differential scattering cross section and has been calculated in Ref. 1.

In order to account approximately for the many-body breakup channels not considered explicitly, we have also introduced into the formulation phenomenological imaginary potentials of the form

$$iW_\lambda(R_\lambda)=-iW_{0\lambda}\left\{\frac{1}{1+e^{(R_\lambda-R_{0\lambda})/a_\lambda}} + \frac{4e^{(R_\lambda-R_{0\lambda})/a_\lambda}}{[1+e^{(R_\lambda-R_{0\lambda})/a_\lambda}]^2}\right\}, \tag{26}$$

where λ denotes either the spin-$\frac{3}{2}$ $d+{}^3$He channel ($\lambda=4$), the spin-$\frac{1}{2}$ $d+{}^3$He channel, or the $p+\alpha$ channel, and the geometry parameters are chosen as

$$\begin{aligned} &R_{04}=R_{0f}=3.5\text{ fm}, \\ &R_{0g}=2.25\text{ fm}, \\ &a_4=a_f=a_g=0.5\text{ fm}. \end{aligned} \tag{27}$$

There are thus three parameters (W_{04}, W_{0f}, and W_{0g}) to be varied at each energy to obtain the best agreement with experimental cross-section results.

III. S MATRIX AND THE LEVEL STRUCTURE OF ^{5}He AND ^{5}Li

A. Determination of exchange–mixture parameter u

In this calculation, the specific distortion effect[9,10] is not considered in the $s=\frac{3}{2}$ state. In the $s=\frac{1}{2}$ state, it is only partially taken into account through the use of two coupled channels. Because of this and other simplifications, it becomes necessary again, as in previous single-channel calculations,[1] to treat the exchange-mixture parameter u in Eq. (12) as an adjustable parameter. Since the spin-$\frac{3}{2}$ and the spin-$\frac{1}{2}$ states are not coupled, we shall adjust the value of u in the spin-$\frac{3}{2}$ state to fit the experimental resonance energies of the $l=0$, $s=\frac{3}{2}$ states in ^{5}He and ^{5}Li, and in the spin-$\frac{1}{2}$ state to yield an over-all good agreement with the empirically determined $n+\alpha$, p-wave phase shifts in the resonance region.

As discussed previously,[1] the above-mentioned procedure leads to a value of u equal to 1.10 in the $s=\frac{3}{2}$ state. For the $s=\frac{1}{2}$ state, the value of u will be chosen to yield a good fit to the $n+\alpha$, p-wave phase shifts calculated using the central part of the optical potential obtained by Satchler *et al.*[11] from a phenomenological study of the experimental data. In Fig. 1, we have plotted the $l=0$ and $l=1$ phase shifts (δ_{0g} and δ_{1g}) as a function of energy for two u values. In this figure, the solid and dashed lines correspond to $u=0.95$ and 0.97, respectively, while the solid dots represent the phase shifts of Satchler *et al.* as described above. For the $l=0$ phase shift, the dashed curve lies slightly above the solid curve, but is too

close to be plotted distinctly. As is seen from this figure, the $l=1$ phase shifts in the resonance region are best fitted with $u=0.95$. This value of u will therefore be used for the $s=\frac{1}{2}$ state in all subsequent discussions.

We should mention that in single-channel resonating-group calculations where the specific distortion effect has not been considered, the value of u required for a particular system seems to be correlated with the compressibility of the clusters involved. Thus, for $\alpha+\alpha$ scattering,[12] where the clusters have a low compressibility, a value of u equal to 0.92 is required, while for the $d+d$ system[7] which consists of two easily compressible clusters, $u=1.2$ yields the best agreement with experiment. For other scattering systems, the values of u lie between these two extreme values. In the $\alpha+{}^3\mathrm{He}$ [6] and ${}^3\mathrm{He}+{}^3\mathrm{He}$ [13] cases, for example, the u values were found to be equal to 0.984 and 1.04, respectively. Thus, it is indeed interesting that in the spin-$\frac{3}{2}$ state, the value of u determined here does fit nicely into this picture.

As has been discussed previously,[10] the specific distortion effect can be taken into account by improving the wave function in the region of strong interaction. This can be achieved either by introducing distortion functions as has been done in the $d+\alpha$ calculation,[10] or by considering more channels as is done in the present case for the $s=\frac{1}{2}$ state. With either of these improvements, one should anticipate that the resultant u value should come closer to 0.92 required in the $\alpha+\alpha$ case where the specific distortion effect has been shown to be relatively unimportant.[14] For the cases so far examined, we have found that this anticipation is in fact well fulfilled. Thus, in the $d+\alpha$ case, the addition of distortion functions has resulted in a value of u equal to 0.925, which is to be compared with the value of 1.175 required in the no-distortion calculation to fit the ground-state binding energy of ${}^6\mathrm{Li}$. Similarly, in the present calculation of the $s=\frac{1}{2}$ state, we find the need of $u=0.95$, which is smaller than the value of $u=0.99$ required in the single-channel $N+\alpha$ problem.[8]

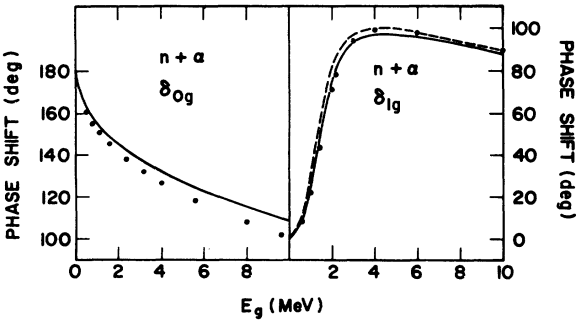

FIG. 1. $n+\alpha$ phase shifts δ_{0g} and δ_{1g} as a function of E_g, calculated with $u=0.95$ (solid lines) and $u=0.97$ (dashed line). The solid dots represent the phase shifts calculated using the central part of the $n+\alpha$ potential empirically determined by Satchler *et al.* (Ref. 11).

B. S matrix elements

Using $u=0.95$ for the $s=\frac{1}{2}$ state, we have computed the $n+\alpha$ phase shifts δ_{lg} up to $l=7$ over a wide range of energies. In order to examine the effect of the $d+{}^3\mathrm{H}$ channel, we have also computed the $n+\alpha$ phase shifts with the coupling kernels k^l_{fg} and k^l_{gf} set equal to zero (single-channel approximation), again using $u=0.95$. In Fig. 2, we compare the coupled-channel phase shifts (solid curves) with the single-channel result (dashed curves) for E_g up to 36 MeV. Evidently, the inclusion of the $d+{}^3\mathrm{H}$ channel has a rather small effect,[15] which is probably due to the fact that the α cluster has a low compressibility and thus is not readily distorted.

We made a similar comparison for the $d+{}^3\mathrm{He}$ phase shifts δ_{lf}. The results in the energy region of E_f from 0 to 16 MeV are shown in Fig. 3, where the coupled-channel phase shifts (solid curves) are seen to be significantly different from the single-channel phase shifts (dashed curves).[16] This is most likely a consequence of the weak binding of the clusters involved. Thus, the additional flexibility obtained through the inclusion of the $p+\alpha$ channel does allow for a significant improvement of the wave function in the strong-interaction region.

The remaining elements of the S matrix are also presented in graphical forms. In Fig. 4 we plot the $p+\alpha$ phase shifts δ_{lg} as a function of E_f, and in Fig. 5 we present the absorption coefficients $(1-\tau_l^2)^{1/2}$. As can be seen from Fig. 5, the reactions $d+{}^3\mathrm{He}\rightleftharpoons p+\alpha$ proceed mainly through the $l=2$ and 3 partial waves in the energy region examined.

Although the $d+{}^3\mathrm{He}$ phase shifts δ_{lf} have changed considerably with the addition of the $p+\alpha$ channel, the odd-even behavior of the phase shift, discussed in Ref. 1, remains; that is, the behavior of the phase shift δ_{lf} is still opposite to the behavior of the phase shift in the spin-$\frac{3}{2}$ state of $d+{}^3\mathrm{He}$. As has been discussed in detail previously,[1] this differing phase-shift behavior in the two spin states is a consequence of the Pauli exclusion principle.

C. Level structure of ${}^5\mathrm{He}$ and ${}^5\mathrm{Li}$

In Ref. 1, an R-matrix analysis of the calculated single-channel $d+{}^3\mathrm{H}$ and $d+{}^3\mathrm{He}$ phase shifts has been performed to determine the level struc-

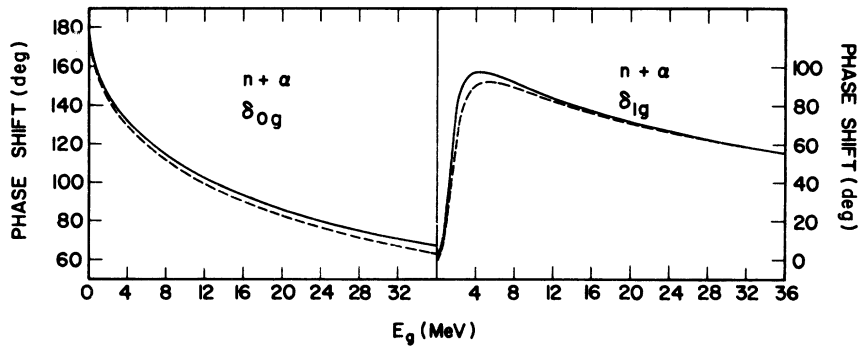

FIG. 2. Comparison of $n+\alpha$ phase shifts δ_{0g} and δ_{1g} obtained with the coupled-channel (solid lines) and the single-channel (dashed lines) calculations.

ture of ^{5}He and ^{5}Li. The levels associated with the spin-$\frac{3}{2}$ state are, of course, not affected by the present calculation. The spin-$\frac{1}{2}$ level structure, on the other hand, is modified. Comparing with Table I of Ref. 1, the present calculation shows that the $l=1$ state is shifted downward by about 0.5 MeV, while the rather broad $l=2$ and 3 levels are shifted upward by about 2.2 and 3.6 MeV, respectively. The major revision comes, however, from the apparent nonexistence of a resonance behavior in the $l=0$ phase shift, as is seen from Fig. 3. At present, the evidence for the possible existence of an $l=0$, $s=\frac{1}{2}$ level in ^{5}He is based on an analysis of the experimental $d+^3$H elastic scattering excitation functions made by Ivanovich, Young, and Ohlsen.[17] In Fig. 6, we plot these experimental excitation functions, together with the predictions of our two-channel calculation. From this figure, one sees that the features of the experimental results are well reproduced.[18] Therefore, the fact that our calculated δ_{0f} shows a smooth, monotonically decreasing behavior indicates that it may be imprudent at this moment to interpret the experimental data as suggesting the presence of a low-energy $l=0$, $s=\frac{1}{2}$ level of $d+^3$H cluster structure.

IV. ELASTIC SCATTERING CROSS SECTIONS

In order to make a comparison with experimental cross-section data, we now introduce phenomenological imaginary potentials into the formulation. This is done by simply replacing V_{Nf} by $V_{Nf}+iW_f$ and V_{Ng} by $V_{Ng}+iW_g$ in Eqs. (15) and (16), and a similar replacement for the direct nuclear potential in the $s=\frac{3}{2}$, $d+^3$He channel. The form of the imaginary potentials is given by Eqs. (26) and (27). There is a total of three adjustable parameters in these potentials, namely, the depth parameters W_{0d}, W_{0f}, and W_{0g}.

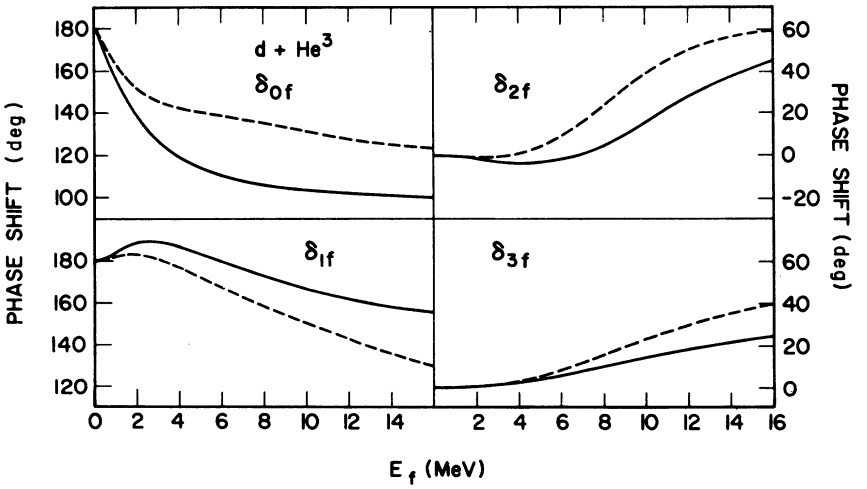

FIG. 3. Comparison of $d+^3$He phase shifts δ_{lf} ($l=0$ to 3) obtained with the coupled-channel (solid lines) and the single-channel (dashed lines) calculations.

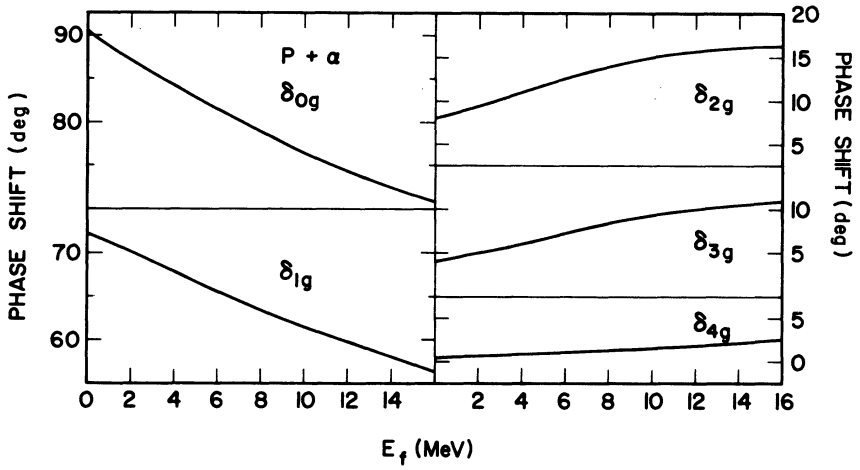

FIG. 4. $p+\alpha$ phase shifts δ_{lg} ($l=0$ to 4) as a function of E_f from 0 to 16 MeV.

In previous single-channel $d+{}^3\mathrm{He}$ [1] and $p+\alpha$ [19] studies, it has been found that the introduction into the imaginary potential of an odd-even orbital-angular-momentum dependence, characterized by a parameter C_I [see Eqs. (14) and (22) of Ref. 1, and Eq. (10) of Ref. 19], has resulted in an improved fit to experiment. In our present calculation we have found, however, that because of the explicit inclusion of a reaction channel, the sensitivity of the calculated cross sections to the parameter C_I is quite weak and a wide range of C_I values, including the value zero, yields rather similar fits to the experimental data. Therefore, since the value of C_I cannot be accurately determined, we have simply chosen to use $C_I=0$, i.e., no odd-even dependence, in this calculation.

The values of W_{04}, W_{0f}, and W_{0g} at various energies are determined by fitting the $d+{}^3\mathrm{H}$ or $d+{}^3\mathrm{He}$ elastic scattering cross-section data[17,20,21] and the $p+\alpha$ total reaction cross-section data.[22] The results are given in Table I, where we have also listed the calculated values of the total reaction cross section σ_R for $d+{}^3\mathrm{H}$ or $d+{}^3\mathrm{He}$ scattering.

The calculation at $E_f=2.02$ MeV merits special attention. At this energy, the parameters W_{0f} and W_{0g} are set equal to zero since no other channels are open, while the parameter W_{04} is adjusted to yield the measured total reaction cross section[20] for $d+{}^3\mathrm{H}$ scattering.[23] The important point to note is, however, that the total reaction cross section and hence, the value of W_{04} is rather small; as a consequence, the calculated $d+{}^3\mathrm{H}$ differential scattering cross section is almost independent of whether W_{04} is chosen as 0.16 MeV or zero. Thus, practically speaking, the calculation at $E_f=2.02$ MeV has no adjustable parameters. In addition,

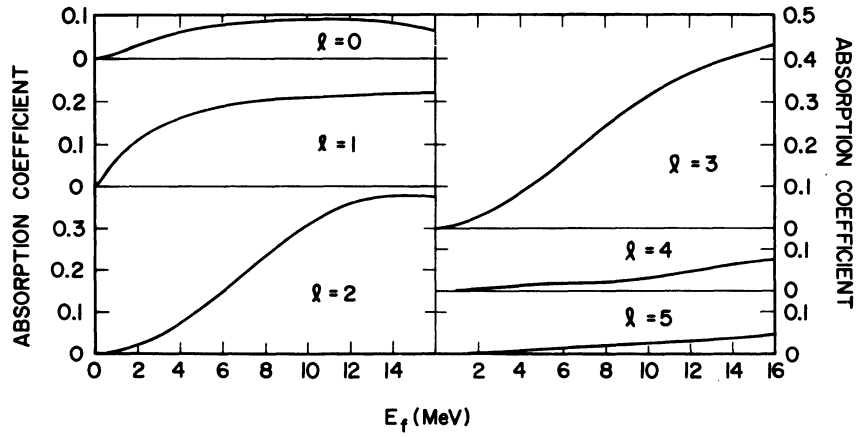

FIG. 5. Absorption coefficients $(1-\tau_l^2)^{1/2}$ as a function of E_f from 0 to 16 MeV.

TABLE I. Imaginary-potential depths W_{04}, W_{0f}, and W_{0g} and total reaction cross sections σ_R for $d+{}^3$H and $d+{}^3$He scattering.

Compound system	E_f (MeV)	E_g (MeV)	W_{04} (MeV)	W_{0f} (MeV)	W_{0g} (MeV)	σ_R (mb)
^{5}He	2.02	21.64	0.16	0	0	80
	4.19	23.81	0.30	0.30	0.30	225
	6.6	26.22	0.45	0.50	0.45	253
^{5}Li	7.23	27.68	0.45	0.60	0.50	250
	8.64	29.09	0.50	0.70	0.55	263
	10.0	30.45	0.55	0.80	0.60	275
	13.84	34.29	0.65	1.00	0.65	285
	17.49	37.94	0.70	1.20	0.70	288

we should mention that in spite of the smaller statistical weighting factor, the spin-$\frac{1}{2}$ contribution to the $d+{}^3$H differential scattering cross section is comparable to the spin-$\frac{3}{2}$ contribution at this energy. Therefore, the result at $E_f = 2.02$ MeV should be particularly useful in illuminating the importance of the explicit inclusion of a reaction channel in a resonating-group calculation.

The results for $d+{}^3$H scattering at 2.02 MeV are shown in Fig. 7. In this figure, the solid and dashed curves represent the results of the present two-channel calculation and the previous one-channel calculation,[1] respectively, while the solid dots represent the experimental data of Ivanovich, Young, and Ohlsen.[17] Here one sees that the two-channel prediction is not only vastly improved over the one-channel prediction, but is also in almost perfect agreement with the experimental result. Thus, it seems that, at least at this energy, our present wave function does give a good description of the behavior of the five-nucleon system.

In Figs. 8 and 9, we show the results of $d+{}^3$H scattering at 4.19 and 6.6 MeV, and of $d+{}^3$He scattering at 8.64, 10.0, and 13.84 MeV. The experimental data[17,20,21] are again plotted as solid dots. Here it is seen that the agreement between calculated and experimental results is very good at 4.19 and 6.6 MeV, fair at 8.64 and 10.0 MeV, and rather poor at 13.84 MeV. As has been mentioned previously,[1] the relatively poor fit at 13.84 MeV may be indicative of the presence of a nearby compound-nucleus resonance level which is not well described by the wave function of this calculation. Also, it is worth mentioning that because, at these higher energies, the spin-$\frac{3}{2}$ contribution to the differential scattering cross sections dominates over the spin-$\frac{1}{2}$ contribution, the difference between the two-channel and one-channel results is not as apparent as that shown in Fig. 7 for $E_f = 2.02$ MeV.

We have also considered $p+\alpha$ elastic scattering in the two-channel approximation. In this case, it is not possible to make a direct comparison with experiment, because a previous single-channel $p+\alpha$ calculation[8] has shown that the large amount of spin-orbit splitting necessitates the addition of a spin-orbit component into the nucleon-

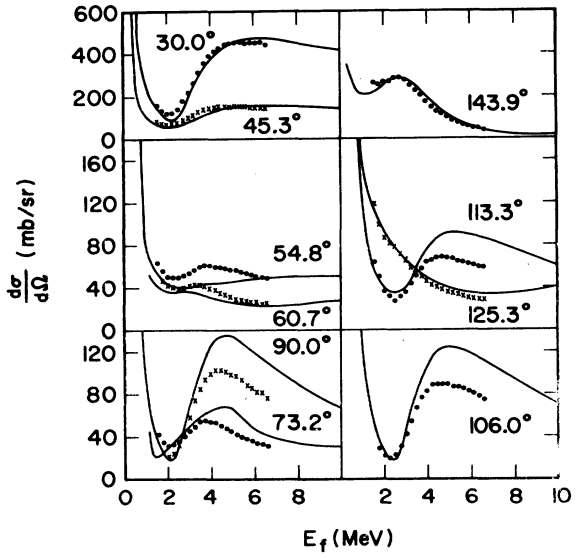

FIG. 6. Comparison of calculated (solid lines) and experimental (solid dots and crosses) excitation functions for $d+{}^3$H scattering. The experimental data are those of Ivanovich, Young, and Ohlsen (Ref. 17).

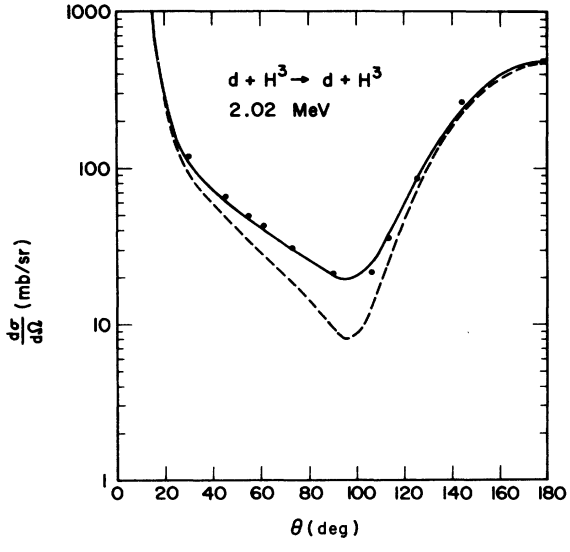

FIG. 7. Comparison of coupled-channel (solid line) and single-channel (dashed line) differential cross sections for $d+{}^3$H scattering at 2.02 MeV with experimental data (solid dots). The experimental data are those of Ivanovich, Young, and Ohlsen (Ref. 17).

nucleon potential.[24] However, this is not a serious drawback, since our primary concern here is not actually fitting experimental data,[25] but to discern the effect of the second channel, which can be done by comparing the two-channel result with the one-channel result, both obtained without a nucleon-nucleon spin-orbit potential. This comparison is shown in Fig. 10 at energies of $E_{\ell}=24.8$ and 36.8 MeV. In this figure, the two-channel result (solid lines) is obtained by using imaginary potentials with values of $W_{0\lambda}$ interpolated from the values given in Table I, while the one-channel result (solid dots) is obtained by first fitting the experimental data of Bunch, Forster, and Kim[26] at 24.8 MeV and Bunker *et al.*[27] at 36.8 MeV with a nucleon-nucleon spin-orbit potential included in the calculation and then leaving this spin-orbit potential off. As is clearly seen, the one-channel and two-channel cross-section predictions are essentially equivalent, indicating again that the specific distortion effect in the $p+\alpha$ system is rather unimportant.

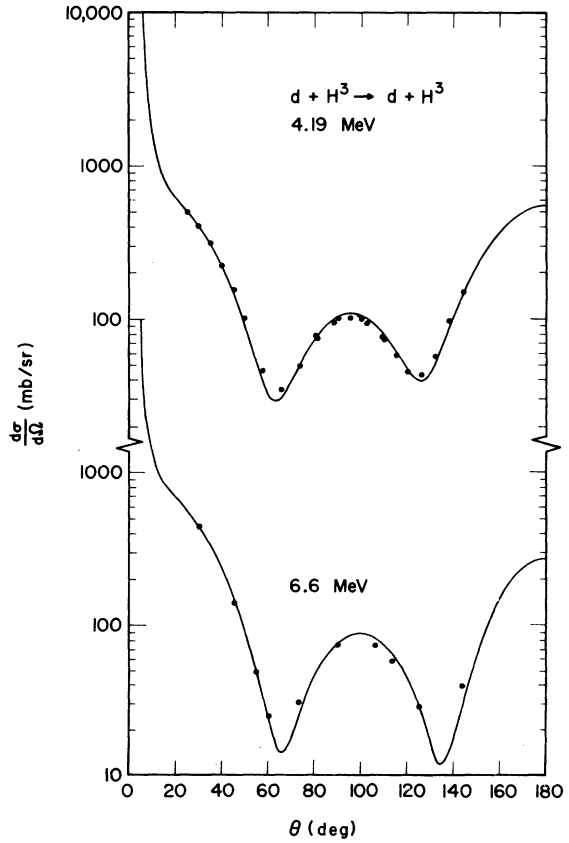

FIG. 8. Comparison of calculated differential cross sections for $d+{}^3\mathrm{H}$ scattering at 4.19 and 6.6 MeV with experimental data. The experimental data are those of Ivanovich, Young, and Ohlsen (Ref. 17).

V. REACTION CROSS SECTIONS

In this section we compare calculated and experimental differential cross sections for the reactions $d+{}^3\mathrm{He}\rightleftarrows p+\alpha$. The effects of other channels will once again be approximated by using imaginary potentials. Since the parameters of these potentials have already been fixed as discussed in Sec. IV (see Table I), no further adjustment will be made in calculating these differential reaction cross sections.

Differential reaction cross sections for the process $d+{}^3\mathrm{He}\rightarrow p+\alpha$ are computed at energies of $E_f=7.23$, 13.84, and 17.49 MeV. The results are

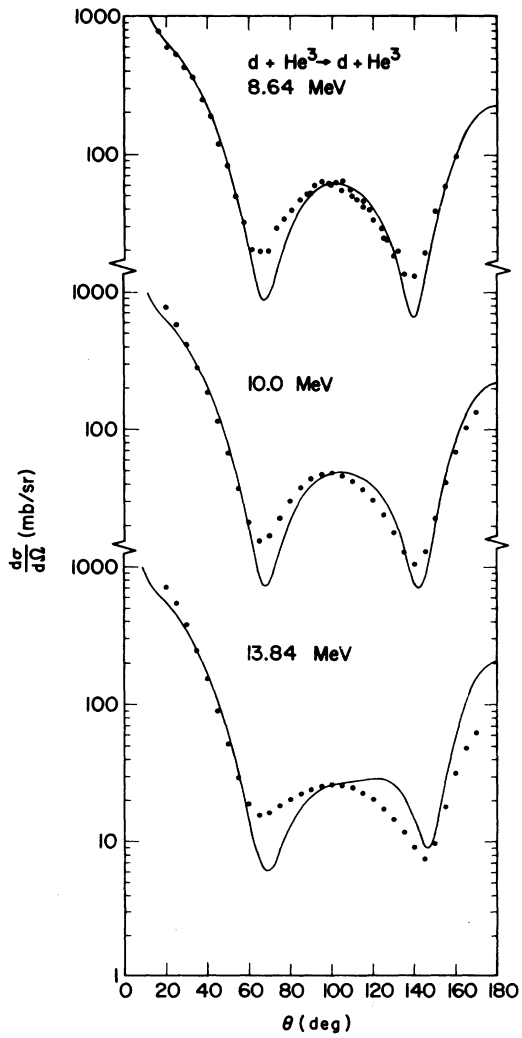

FIG. 9. Comparison of calculated differential cross sections for $d+{}^3\mathrm{He}$ scattering at 8.64, 10.0, and 13.84 MeV with experimental data. The experimental data at 8.64 MeV are those of Brolley *et al.* (Ref. 20); and at 10.0 and 13.84 MeV are those of King and Smythe (Ref. 21).

shown in Fig. 11, together with the experimental data (solid dots) of King and Smythe.[21] From this figure, one notes that the general features of the experimental angular distributions are well reproduced. In particular, there is good agreement between the calculated and experimental angles at which the maxima and minima occur.

The major discrepancy between theory and experiment is that the calculated cross sections are somewhat too small.[28] The reasons for this are probably as follows:

(i) The rms radii of the clusters (d and ^{3}He) in the incident channel are quite different from the rms radius of the cluster (α) in the outgoing channel. Consequently, one expects that the transition probability between these channels will be relatively small and sensitive to the behavior of the wave function in the strong-interaction region. To investigate this possibility, one could, for example, systematically add more and more five-nucleon wave functions of the bound-state type (distortion functions) with linear variational amplitudes into the wave function of Eq. (1), and examine the sensitivity of the calculated cross sections with respect to these additions.

(ii) There is no coupling between the $s=\frac{3}{2}$, $d+^3$He channel and the $p+\alpha$ channel in our calculation. This will obviously cause some underestimate of the reaction cross sections. As a remedy for this, one clearly needs to add noncentral components into the nucleon-nucleon potential of Eq. (12).

To carry out these improvements would obviously require a great deal of effort; however, with some simplifications, such as the use of a relatively simple nucleon-nucleon spin-orbit potential, we

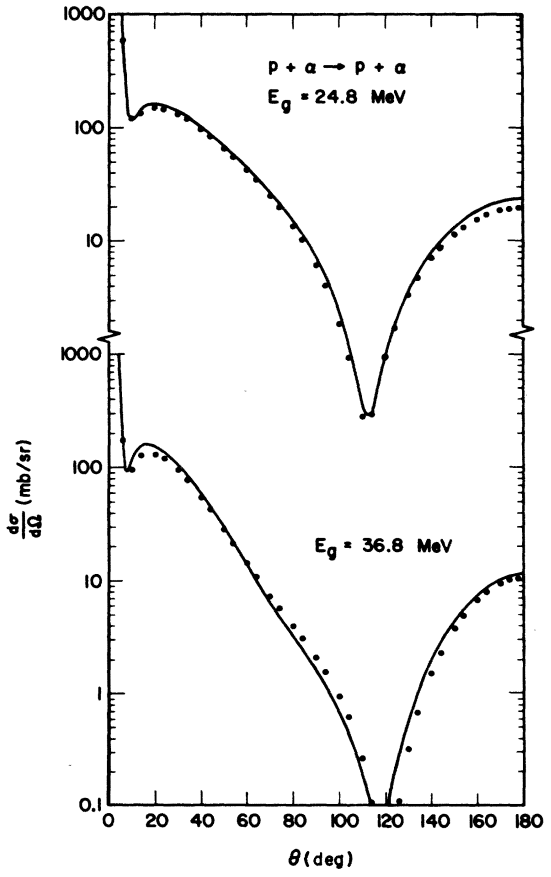

FIG. 10. Comparison of coupled-channel (solid lines) and single-channel (solid dots) differential cross sections for $p+\alpha$ scattering at 24.8 and 36.8 MeV.

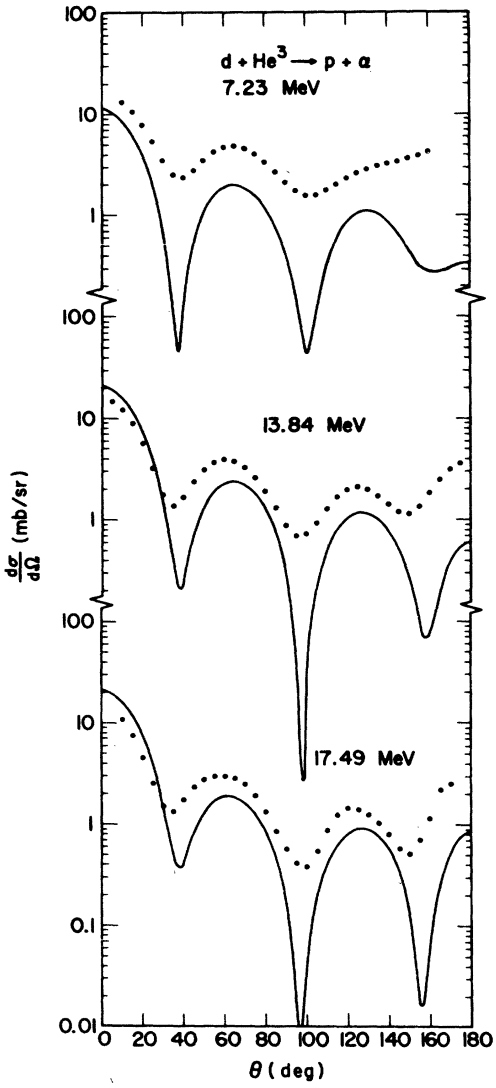

FIG. 11. Comparison of calculated differential cross sections for the process $d+^3$He$\rightarrow p+\alpha$ with experiment at 7.23, 13.84, and 17.49 MeV. The experimental data are those of King and Smythe (Ref. 21).

feel that the task will certainly be a feasible one.

In order to see the effect of the imaginary potentials, we compare, in Fig. 12, the $d+{}^3\mathrm{He} \rightarrow p+\alpha$ differential reaction cross sections at $E_f = 10$ MeV calculated with (solid curve) and without (dashed curve) imaginary potentials. The experimental data shown are again those of King and Smythe.[21] As expected one finds that the inclusion of the imaginary potentials merely alters the magnitude of the cross section, but does not affect the main features.

Finally, we have computed the $p+\alpha \rightarrow d+{}^3\mathrm{He}$ differential reaction cross section at $E_g = 68$ MeV, with $W_{0f} = 1.7$ MeV and $W_{0g} = 1.0$ MeV.[29] The result (solid curve) is shown in Fig. 13, together with the experimental data (solid dots) of Votta *et al.*[30] Here we see that even at this relatively high energy, the agreement between calculation and experiment is still quite satisfactory.

VI. CONCLUSION

In this investigation, we have made a coupled-channel study of the five-nucleon system using the resonating-group method. The channels which are explicitly considered are the $d+{}^3\mathrm{He}$ (or $d+{}^3\mathrm{H}$) and the $p+\alpha$ (or $n+\alpha$) channels. Three- and more-body breakup channels are not included in this calculation, but their effects have been crudely taken into account by the introduction of phenomenological imaginary potentials into the formulation.

One of the purposes of this investigation is to see the effect of the introduction of a second channel. The result shows that while the $p+\alpha$ phase shifts are essentially unaffected by the addition of the $d+{}^3\mathrm{He}$ channel, the coupled-channel $d+{}^3\mathrm{He}$ phase shifts are significantly different from the phase shifts predicted by the single-channel calculation.

The substantial difference between the single-channel and coupled-channel $d+{}^3\mathrm{He}$ (or $d+{}^3\mathrm{H}$) phase shifts makes it necessary to modify our previous conclusion[1] about the level structure of ${}^5\mathrm{Li}$ (or ${}^5\mathrm{He}$) in the spin-$\frac{1}{2}$ state. Comparing with the level positions given in our previous publication,[1] the $l=1$ state is shifted downward by about 0.5 MeV, while the rather broad $l=2$ and 3 states are shifted upward by about 2.2 and 3.6 MeV, respectively. The major revision comes, however, from the observation that the $l=0$, $s=\frac{1}{2}$ phase shift obtained here has a smooth, monotonically decreasing behavior. This indicates that there may not be an $l=0$, $s=\frac{1}{2}$ level at an energy close to the $d+{}^3\mathrm{He}$ (or $d+{}^3\mathrm{H}$) threshold, as reported previously.[1]

With phenomenological imaginary potentials in the formulation, we have also calculated differential elastic scattering and reaction cross sections at various energies. For the $d+{}^3\mathrm{He}$ and $p+\alpha$ differential scattering cross sections, we have found that the calculated results agree in general quite well with the experimental data. As for the

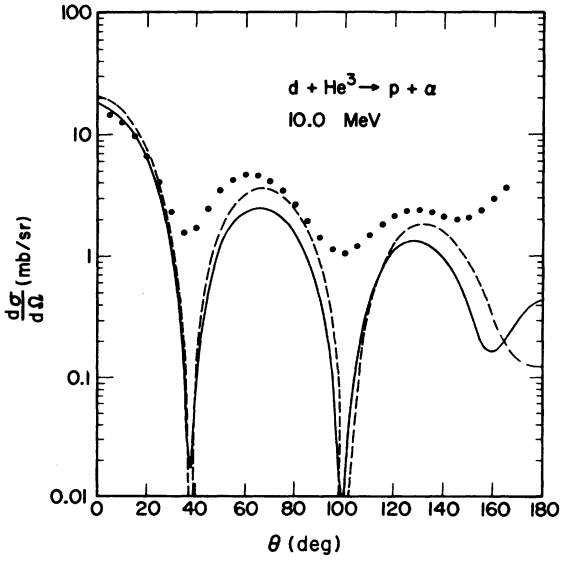

FIG. 12. Comparison of differential reaction cross sections for the process $d+{}^3\mathrm{He} \rightarrow p+\alpha$ at 10 MeV calculated with (solid line) and without (dashed line) imaginary potentials. The experimental data shown are those of King and Smythe (Ref. 21).

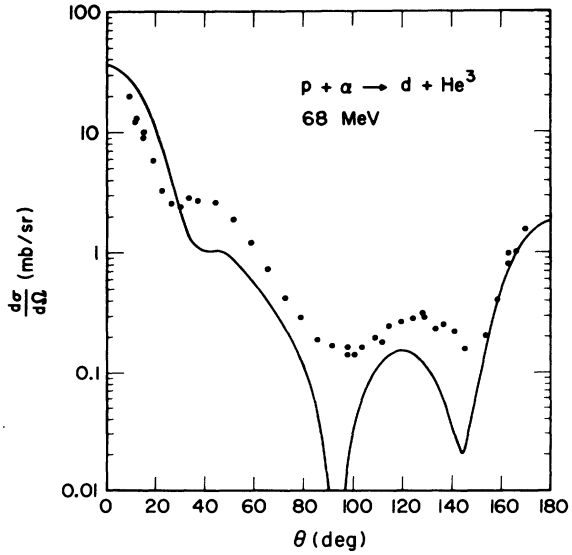

FIG. 13. Comparison of calculated differential reaction cross section for the process $p+\alpha \rightarrow d+{}^3\mathrm{He}$ with experiment at 68 MeV. The experimental data are those of Votta *et al.* (Ref. 30).

$d + {}^3\mathrm{He} \rightleftarrows p + \alpha$ differential reaction cross sections, the comparison between theory and experiment is somewhat less satisfactory. Thus, while the main features of the experimental angular distributions are well reproduced, the magnitude of the calculated cross section is somewhat too low.

Even though the results are generally quite satisfactory, there are a number of improvements which should be made in future calculations. These improvements are:

(i) The adoption of a trial wave function which is more flexible in the strong-interaction region. This can be achieved in both the $s = \frac{3}{2}$ and $s = \frac{1}{2}$ states by the introduction of five-nucleon bound-state-type wave functions with linear variational amplitudes.

(ii) A proper consideration of the coupling between the $s = \frac{3}{2}$ channel and the $s = \frac{1}{2}$ channels. An obvious way to do this is the addition of noncentral components into our presently adopted nucleon-nucleon potential.

(iii) A better value for the $d + {}^3\mathrm{He}$ or $d + {}^3\mathrm{H}$ threshold energy. We can obtain this by improving the binding-energy value of the three-nucleon cluster through the use of a more flexible two-Gaussian spatial wave function.

Finally, we should mention that the formulation obtained here can be used to examine various reaction mechanisms, such as stripping processes and so on. By studying the contribution to the differential reaction cross section of the various terms in the coupling kernel functions, it is our hope that one can thereby learn the roles played by these reaction mechanisms in the forward and backward angular regions.[31]

The authors wish to thank Professor N. Chant for the permission to use his experimental results prior to publication.

---

*Work supported in part by the U. S. Atomic Energy Commission.

†Present address: Department of Physics, Florida State University, Tallahassee, Florida 32306.

[1]F. S. Chwieroth, R. E. Brown, Y. C. Tang, and D. R. Thompson, Phys. Rev. C 8, 938 (1973), and references contained therein.

[2]W. Laskar, C. Tate, B. Pardoe, and P. G. Burke, Proc. Phys. Soc. Lond. 77, 1014 (1961).

[3]P. Heiss and H. H. Hackenbroich, Nucl. Phys. A162, 530 (1971).

[4]J. E. A. Lys and L. Lyons, Nucl. Phys. 74, 261 (1965).

[5]F. S. Chwieroth, Ph. D. thesis, University of Minnesota, 1973 (unpublished); University of Minnesota Report No. COO-1764-180 (unpublished).

[6]J. A. Koepke, R. E. Brown, Y. C. Tang, and D. R. Thompson, to be published; I. Reichstein, D. R. Thompson, and Y. C. Tang, Phys. Rev. C 3, 2139 (1971).

[7]F. S. Chwieroth, Y. C. Tang, and D. R. Thompson, Nucl. Phys. A189, 1 (1972).

[8]I. Reichstein and Y. C. Tang, Nucl. Phys. A158, 529 (1970).

[9]H. Jacobs, K. Wildermuth, and E. Wurster, Phys. Lett. 29B, 455 (1969).

[10]D. R. Thompson and Y. C. Tang, Phys. Rev. C 8, 1649 (1973).

[11]G. R. Satchler, L. W. Owen, A. J. Elwyns, G. L. Morgan, and R. L. Walter, Nucl. Phys. A112, 1 (1968).

[12]R. E. Brown and Y. C. Tang, Nucl. Phys. A170, 225 (1971).

[13]D. R. Thompson, Y. C. Tang, J. A. Koepke, and R. E. Brown, Nucl. Phys. A201, 301 (1973).

[14]L. C. Niem, P. Heiss, and H. H. Hackenbroich, Z. Phys. 244, 346 (1971).

[15]Similar conclusion holds for phase shifts with $l \geq 2$.

[16]Higher-l, $d + {}^3\mathrm{He}$ phase shifts in the coupled-channel calculation differ by only a few degrees from those in the single-channel calculation.

[17]M. Ivanovich, P. G. Young, and G. G. Ohlsen, Nucl. Phys. A110, 441 (1968).

[18]In the energy region above 3 MeV, the calculated cross sections are generally too large. This is because no imaginary potential has been included to obtain the results discussed here or elsewhere in Sec. III.

[19]D. R. Thompson, Y. C. Tang, and R. E. Brown, Phys. Rev. C 5, 1939 (1972).

[20]J. E. Brolley, Jr., T. M. Putnam, L. Rosen, and L. Stewart, Phys. Rev. 117, 1307 (1960).

[21]T. R. King and R. Smythe, Nucl. Phys. A183, 657 (1972).

[22]The $p + \alpha$ total reaction cross-section values are taken from Table I of Ref. 19, where the experimental sources are quoted. In addition, it should be mentioned that a recent measurement of $p + \alpha$ total reaction cross sections by A. Sourkes *et al.* (private communication to R. E. Brown) at the University of Manitoba agrees with the σ_R results given in that table.

[23]From a phenomenological viewpoint, it is necessary to choose a nonzero value for W_{04}. Even though no transition is allowed between the $s = \frac{3}{2}$, $d + {}^3\mathrm{H}$ channel and the $n + \alpha$ channel in our model, such transition does occur in actuality.

[24]It has been shown by Heiss and Hackenbroich (Ref. 3) that the amount of spin-orbit splitting in the $d + {}^3\mathrm{He}$ phase shifts is rather small.

[25]This can already be done in the single-channel approximation (Ref. 8) by including a nucleon-nucleon spin-orbit potential.

[26]S. M. Bunch, H. H. Forster, and C. C. Kim, Nucl. Phys. 53, 241 (1964).

[27]S. N. Bunker, J. M. Cameron, M. B. Epstein, G. Paic, J. R. Richardson, J. Rogers, P. Thomas, and J. W. Verba, Nucl. Phys. A133, 537 (1969).

[28]The ratios of the calculated and experimental differential reaction cross sections at the first maximum of around 65° are equal to 0.42, 0.55, 0.62, and 0.65 at energies of 7.23, 10.0, 13.84, and 17.49 MeV, respectively.

[29]These values are obtained by using the $p+\alpha$ differential scattering cross-section data of L. G. Votta, P. G. Roos, N. S. Chant, and R. Woody, III [University of Maryland Technical Report No. 74-011, 1973 (unpublished)] and by making a smooth but not unique extrapolation of the values given in Table I. We shall be able to make a better determination of W_{0f} and W_{0g} when the $d+{}^3$He differential scattering and total reaction cross sections at this energy become available.

[30]Votta, Roos, Chant, and Woody (see Ref. 29); N. S. Chant, private communication.

[31]Such a study for the process ${}^3\mathrm{He}+{}^4\mathrm{He}\rightarrow p+{}^6\mathrm{Li}$ has been carried out recently by R. Hub, D. Clement, and K. Wildermuth, Z. Phys. 252, 324 (1972).